THE ASTROPHYSICAL JOURNAL, 331:1013–1028, 1988 August 15


# RADIAL AND NONRADIAL PULSATIONS OF POLYTROPES: HIGH-PRECISION EIGENVALUES AND THE APPROACH OF *p*-MODES TO ASYMPTOTIC BEHAVIOR

D. J. MULLAN
Bartol Research Institute, University of Delaware

AND

R. K. ULRICH
Astronomy Department, University of California at Los Angeles
*Received 1987 December 14; accepted 1988 February 9*

## ABSTRACT

In order to extract eigenfrequencies of high-order *p*-modes with precisions of one part in 500,000, a careful numerical treatment is necessary for both the input stellar model and the oscillation code. Here, we use polytropes to avoid uncertainties associated with the input model. We have obtained eigenfrequencies in a number of polytropes for *l*-values of 0–3 and radial orders up to about 40. In order to have the frequencies converge with the necessary precision, we find that the input model must contain several thousand shells, and the oscillation code must contain at least several dozen grid points in each loop of the eigenfunction. The outermost loop requires many more points: our converged models contain several hundred grid points between the last node and the surface.

An important check on our results is provided by a comparison of the asymptotic behavior of adjacent mode separations with the limiting behavior predicted by Tassoul. Our oscillation code is based on the Cowling approximation (as assumed by Tassoul).

*Subject headings:* stars: pulsation — Sun: oscillations

## I. INTRODUCTION

Radial and nonradial pulsations of the Sun and stars hold the key to the rapidly growing fields of helioseismology and asteroseismology. As the GONG project comes on line in the next few years, the frequencies of solar pulsation modes will be measured with increasingly high precision, of order 0.01 $\mu$Hz. In the frequency range where solar oscillations have so far been detected with maximum power (roughly 1.7–5 mHz), this corresponds to a fractional uncertainty of $2 \times 10^{-6}$ in the mode frequencies. The radial order of the observed modes can be as high as 40.

A major theoretical challenge will be the ability to predict the eigenfrequencies of a solar model with precisions of the above order. Difficulties in meeting this challenge arise from two separate sources. First, current solar models are subject to uncertainties arising from opacities and treatment of convection which are much larger (fractionally) than the above requirements. Second, the codes which extract the oscillation frequencies are subject to numerical errors. In the present paper, we are concerned only with the second of these.

As a means of checking an oscillation code, it is convenient to refer to a test model "star" in which the structure is known with essentially infinite precision. Polytropes provide such test models. Eigenfrequencies for some low-order modes in certain polytropes exist in the literature (e.g., Cox 1980). But these are inadequate for present purposes for two reasons. First, the numerical precision is typically poorer than we require by several orders of magnitude. Second, they do not provide a really stringent test of an oscillation code: the eigenfunctions of the low-order modes do not oscillate rapidly near the surface of the star and therefore do not require the careful treatment that is necessary for modes of high order. In a more recent discussion, Christiansen-Dalsgaard (1982) has obtained eigenfrequencies for some high-order *p*-modes for the $n = 3$ and $n = 0$ polytropes: however, at the highest orders which he gives (radial order 30), the fractional errors in the eigenfrequencies fall short of the required precision by one to two orders of magnitude. (The uncertainties are much smaller for the lower order modes, but such modes carry very little power in the solar oscillation spectrum.)

An important check on our eigenfrequency results is provided by the asymptotic behavior of the *p*-modes at high frequency. Tassoul (1980) has discussed at length how the frequency separation of high-order *p*-modes is expected to behave asymptotically. Tassoul's results have recently been rediscussed including higher order terms by Smeyers and Tassoul (1987), but the earlier results of Tassoul (1980) are of sufficiently high order to be relevant here. According to Tassoul (1980),

$$\nu_{n_r,l} = \alpha + \beta(x - x_0) \tag{1}$$

where

$$x = n_r + \frac{l}{2}. \tag{2}$$

Here, $n_r$ is the radial order of the mode; $l$ is the degree of the spherical harmonic, equaling the number of complete circles on which the vertical component of the velocity of oscillation is always zero;

$$\alpha = \alpha_0 - \alpha_1 l(l+1) \tag{3}$$

and

$$\beta = \beta_0 + \beta_1 l(l+1) \tag{4}$$

The notation in equations (3) and (4) is that of Gough (1984).

We note that although the radial order $n_r$ equals the number of radial nodes in polytropes which are not too centrally condensed, this is no longer true for highly condensed polytropes: in the latter, it may be necessary to exclude modes which oscillate in the $g$-propagation region (Robe 1968; Scuflaire 1974). Numerical values of $\alpha_0$ and $\beta_0$ are sensitive to the physical structure of the outer layers of the polytrope; the numerical values of $\alpha_1$ and $\beta_1$ are also sensitive to physical conditions in the core. As the mode number increases, the asymptotic frequency separation between successive modes ($n_r$ and $n_{r+1}$) is given by the quantity $\beta$. The limiting value of the mode separation is related to the sound travel time between surface and center:

$$\beta_0^{-1} = 2 \int_0^R \frac{dr}{c_s}, \tag{5}$$

where $c_s$ is the sound speed.

The existence of asymptotic behavior has an important computational advantage: the higher the order of the pulsation mode, the more grid points are required in order to compute the frequency with a specified precision. Thus, a considerable saving of computational effort would result if the asymptotic behavior of the frequences could be relied upon.

One of the questions we address in the present paper is: how reliable is the asymptotic behavior in practice? For example, how large does the radial node number need to be in order to have, say, successive mode frequencies separated by an amount which equals the asymptotic limit ($\beta$) with a precision comparable to that which the GONG observers will be achieving, i.e., 0.01 $\mu$Hz?

To address this question, we restrict our attention in this paper (for the sake of consistency) to the particular case for which Tassoul originally derived the asymptotic behavior: that is, we consider only pulsations which are described by the Cowling approximation (i.e., neglecting variations in gravitational potential in the course of the pulsation).

## II. RADIAL AND NONRADIAL PULSATIONS OF POLYTROPES

The characteristic Lamb frequencies $L$ and Brunt-Vaisala frequencies $N$ (in the notation of Unno *et al.* 1981) associated with restoring forces of pressure and gravity in a polytrope of order $n$ can be calculated as functions of radius in terms of the Lane-Emden function $\theta$. For the definition of $\theta$, see, e.g., Chandrasekhar (1939): in a perfect gas, $\theta$ equals the ratio of local temperature to central temperature. The dimensionless radial coordinate $\xi$ is related to the radial variable $r$ by $\xi = r/r_n$, where $r_n$ is the Emden unit of length.

Thus, if we define

$$\omega_g^2 = \frac{GM}{R^3}, \tag{6}$$

where $M$ and $R$ are mass and radius, and $G$ is the gravitational constant, we can write a normalized Brunt-Vaisala frequency (subscript $n$ denotes normalization) as

$$N_n^2 \equiv \frac{N^2}{\omega_g^2} = \frac{(n - n_0)}{(n_0 + 1)} \times CC \times \left(\frac{3\theta'^2}{\theta}\right) \tag{7}$$

where $CC$ is the central condensation of the polytrope (i.e., central density divided by mean density). The parameter $n_0$ is the effective polytropic index associated with the pulsations. In all models to be described here, we have taken $n_0 = 1.5$: the associated adiabatic exponent

$$\Gamma = 1 + \frac{1}{n_0} \tag{8}$$

has the value 5/3 in all of our results. In equation (7), prime denotes differentiation with respect to $\xi$.

Similarly, the value of $L$ associated with mode l is given by

$$L_{ln} \equiv \frac{L_l^2}{\omega_g^2} = 3 \times CC \times l(l+1) \times \frac{\theta}{\xi^2} \times \frac{(n_0 + 1)}{n_0(n+1)}, \tag{9}$$

where $\xi$ is the Lane-Emden coordinate.

The quantity $N_n$ diverges at the surface, and $L_n$ diverges at the center. As will be mentioned below, our integrations are terminated at a radial distance slightly beneath the formal surface: as a result, the divergence in $N_n$ is avoided. Near the center, we avoid the divergence in $L_n$ by starting the integrations at a finite (but small) value of $\xi$, typically at a fractional radius of a few times $10^{-4}$.

With regard to the increase in $N_n$ near the surface, for future reference we note that at a certain radial distance, $\xi_N$, the value of $N_n$ becomes equal to the normalized eigenfrequency, $\omega_n$. The value of $\theta$ at this variable transition point (in the notation of Tassoul 1980) will be denoted by $\theta_N$. An equivalent variable transition point also exists near the center of the polytrope (if $l \neq 0$), where $L_n$ becomes equal to $\omega_n$.

### a) *Standard Frequency*

In the calculations to be reported below, we restrict attention to a polytrope of solar mass and radius. Taking $M = 1.989 \times 10^{33}$ g, $R = 6.9627 \times 10^{10}$ cm, and $G = 6.67 \times 10^{-8}$ cgs, we use the following standard frequency in the results:

$$\nu_g \equiv \frac{\omega_g}{2\pi} = 99.778\ \mu\text{Hz}. \tag{10}$$

If other choices of constants are preferred, our results can be scaled accordingly. For example, if one prefers the product $GM = 1.32712438 \times 10^{26}$ cgs based on planetary motion, the standard frequency (assuming the same value for $R$ as above) would become 99.795 $\mu$Hz. All of our frequencies should then be multiplied by a factor 1.000174.

Another unit of frequency to which we shall refer below is $\nu_s$: this is the ratio of the sound speed at the center of the star to the Emden unit of length. The ratio of $\nu_s$ to $\nu_g$ is $2\pi[3\Gamma \times CC/(n+1)]^{1/2}$.

### b) *Polytrope Structure*

We use a fourth-order Runge-Kutta method to solve the Lane-Emden equation with variable step size. The output from the structure integration is a table of $N_r$ values of the frequencies $\log N^2$ and $\log L^2$. The number of radial grid points $N_r$ which we have used in our solutions ranges over almost an order of magnitude, from several hundred to several thousand. Oscillation frequencies are extracted from each radial grid set until it becomes clear that increasing the number of grid points in the input polytrope table no longer causes the eigenfrequency to alter by more than 0.01 $\mu$Hz.

The "surface" of the polytrope, where the Lane-Emden function $\theta$ passes through the value $\theta = 0$ for the first time, lies formally at a well-defined value of $\xi = \xi_1$ (Chandrasekhar

1939). However, in order to avoid singularities in our numerical treatment of oscillations, we truncate the polytrope model at an artificial "surface," where $\theta$ has a finite nonzero value, $\theta_0$. We will discuss below the effect which the choice of $\theta_0$ has on the eigenfrequencies. The major requirement is that $\theta_0$ must be less than the value at the variable transition point $\theta_N$ as defined above. For high-frequency modes, this requires that $\theta_0$ be chosen to have a very small value. In almost all of the results to be presented below, we have used $\theta_0 = 10^{-8}$. (Exceptions will be noted.) Thus, for a model where the central temperature is equal to the solar value (about $10^7$ K), our typical cutoff occurs at a radial distance from the center of the star where the local temperature has fallen to about 0.1 K. For the $n = 3$ polytrope, this cutoff is located at a fractional radial distance of $3.4 \times 10^{-8}$ beneath the formal surface: in the Sun, this corresponds to a depth of 0.024 km. For $n = 0$, we used $\theta_0 = 10^{-6}$ because of numerical difficulties associated with the step in density at the surface.

The asymptotic frequency separation between successive $p$-modes for polytrope $n$ can be written as follows:

$$\beta_0 = \sqrt{5G\frac{M}{4R^3}} \times \frac{1}{\xi_1} \times \sqrt{\frac{CC}{n+1}} \times \frac{1}{I_0}, \tag{11}$$

where

$$I_0 = \int_0^1 \frac{df}{\sqrt{\theta}}. \tag{12}$$

In the integral on the right-hand side, the upper limit is formally unity, and $f$ is the radial coordinate expressed in terms of the radius of the star:

$$f \equiv \frac{\xi}{\xi_1}. \tag{13}$$

In view of the cutoff which we have imposed on the integration to avoid divergence at the surface ($\theta = \theta_0$), the practical upper limit in the integral in equation (12) is slightly less than unity, $1 - f_0$. Note that $\beta_0 \xi_1 I_0 = v_s/2$.

Inserting the choices of $G$, $M$, and $R$ mentioned above, the numerical coefficient on the right-hand side of the expression for $\beta_0$ has the value 700.92 $\mu$Hz. Using this, we find that for each polytrope, we can write

$$\beta_0 = \frac{C_n}{I_0(n)}. \tag{14}$$

Values of $C_n$ are listed in Table 1 for a representative number of polytropes.

The value of $I_0$ can be obtained analytically for the case $n = 0$ without any cutoff near the surface: $I_0(0) = \pi/2$. Evaluating the integral with the cutoff of $\theta_0 = 10^{-6}$ in this case, we found $I_0(0) = 1.56942$, i.e., fractionally smaller than the correct value by $8.8 \times 10^{-4}$. Also for $n = 0$, the complete oscillation problem (including the gravitational potential perturbations) has eigenvalues which approach asymptotic separations of $(2\Gamma)^{1/2}$ in units of the standard frequency (Pekeris 1938). Using the standard frequency mentioned above (99.778 $\mu$Hz), this corresponds to asymptotic separations of 182.17 $\mu$Hz. In the asymptotic limit, this is also expected to be valid for the Cowling approximation: compared with our value of 182.33 (see Table 1), the fractional difference ($8.8 \times 10^{-4}$) can be attributed in its entirety to our cutoff at a finite value of $\theta$.

For other values of $n$, the integral $I_0$ was performed numerically, using the cutoff mentioned above at $\theta_0 = 10^{-8}$. Combining these with the values of $C_n$ we obtain the corresponding values of $\beta_0(\theta_0)$ in Table 1.

TABLE 1

CHARACTERISTIC FREQUENCIES IN POLYTROPES

| Polytrope Index | $C_n$ | $\theta_0$ | $\beta_0(\theta_0)$ | $\beta_0(0)$ |
|---|---|---|---|---|
| 0.0 ..... | 286.15 | $10^{-6}$ | 182.33 | 182.17 |
| 1.0 ..... | 286.15 | $10^{-8}$ | 152.58 | 152.57 |
| 1.5 ..... | 296.96 | $10^{-8}$ | 143.31 | 143.29 |
| 2.0 ..... | 313.93 | $10^{-8}$ | 135.71 | 135.69 |
| 3.0 ..... | 374.03 | $10^{-8}$ | 123.53 | 123.50 |
| 3.25 ..... | 398.09 | $10^{-8}$ | 120.91 | 120.88 |
| 3.5 ..... | 428.44 | $10^{-8}$ | 118.42 | 118.38 |
| 4.0 ..... | 522.34 | $10^{-8}$ | 113.75 | 113.71 |
| 4.25 ..... | 602.69 | $10^{-8}$ | 111.55 | 111.52 |
| 4.5 ..... | 738.57 | $10^{-8}$ | 109.42 | 109.36 |

NOTE. Frequency units: $\mu$Hz; standard frequency 99.778 $\mu$Hz.

Note that the deeper the cutoff is located beneath the "true" surface, the larger the numerical value of $\beta_0(\theta_0)$ becomes. As an indication of the sensitivity of $\beta_0$ to the choice of cutoff, we find that for $n = 3$, if we alter the cutoff to $\theta_0 = 10^{-k}$, where $k = 4$, 5, 6, and 7, the corresponding values of $\beta_0$ are found to be 126.35, 124.38, 123.77, and 123.58 $\mu$Hz, respectively. These are to be compared with 123.53 $\mu$Hz for $k = 8$ (Table 1).

For sufficiently small values of $\theta_0$, the subsurface cutoff depth $(1 - f_0)$ becomes directly proportional to $\theta_0$: for example, with $n = 3$, we find

$$(1 - f_0) \approx 3.4 \times \theta_0. \tag{15}$$

Thus, with $n = 3$, the subsurface depth of the cutoff with $k = 5$ is 24 km. As a result, cutting off the $n = 3$ polytrope at even a few dozen kilometers beneath the surface will result in overestimates of order 1 $\mu$Hz in the asymptotic mode separation.

Using the proportionality between $\theta_0$ and the cutoff depth near the surface, we can extend the numerical integration of $I_0$ analytically to the true surface. For $n = 3$ we find the "true asymptotic" value to be

$$\beta_0(0) = 123.50\ \mu\text{Hz}. \tag{16}$$

Values of the "true asymptotic" mode separations are listed for all of the polytropes in Table 1 as $\beta_0(0)$. It is apparent that if the asymptotic mode separation is to be obtained with a value which agrees with the true asymptotic value within 0.01 $\mu$Hz, the subsurface cutoff must be chosen at even smaller values of $\theta_0$ than we have used here. [For example, a value of $10^{-10}$ is required for $\theta_0$ if $\beta_0(\theta_0)$ is to be within 0.01 $\mu$Hz of the "true asymptotic" value for $n = 3$.] However, because of computational limitations, we have not attempted in this paper to place the cutoff depth closer to the surface than $\theta_0 = 10^{-8}$. The point is that, whatever value one chooses for the cutoff level, for consistency the numerical mode separations should approach the value of $\beta_0$ corresponding to that cutoff.

### c) *Oscillation Code*

Following Cowling (1941), the oscillation variables $w$ and $z$ (associated with the pressure perturbation and the radial component of the displacement, respectively) at angular frequency $\omega$ satisfy the equations

$$\frac{dw}{d\xi} = \frac{n+1}{3CC} \times z \times \theta^{-Q} \times (\omega_n^2 - N_n^2) \tag{17}$$

and

$$\frac{dz}{d\xi} = -\left(\frac{2z}{\xi}\right) + \left(\frac{3CC}{n+1}\right) l(l+1)\left(\frac{w}{\xi^2}\right)\theta^Q \quad \left(\frac{1}{\omega_n{}^2} - \frac{1}{L_{\ln}{}^2}\right). \quad (18)$$

Here, frequences with subscript "$n$" denote normalization relative to $\omega_g$, and $Q = (n + 6)/5$ for our choice of $n_0$.

We integrate these two equations from center to "surface" by a fourth-order Runge Kutta method, where by "surface" we denote the radial distance where $\theta = \theta_0$. In the oscillation code, the tabulated logarithmic values of $N_n$ and $L_n$ are interpolated linearly in the radial coordinate 3 times for each radial step.

i) *Integration near the Center*

In order to ensure maximum precision in the eigenfrequencies, we begin the integration near $\xi = 0$ using eigenfunctions which are extracted from equations (17) and (18) by retaining only the dominant term in the coefficients of $z$ and $w$ in these equations. For $l \neq 0$, the (unnormalized) dominant terms are found to be

$$z = \xi^{l-1} \quad (19)$$

and

$$w = (A/l) \times \xi^l , \quad (20)$$

where

$$A = \frac{n+1}{3CC} \times \omega_n{}^2 . \quad (21)$$

The functional form of equation (19) is consistent with the findings of Smeyers and Tassoul (1987) that the radial component of the displacement at the center of the star is finite and nonzero for $l = 1$ and zero for $l > 1$. For $l = 0$, the dominant terms are found to be

$$w = \exp - A\frac{\xi^2}{6\Gamma} \quad (22)$$

and

$$z = -\frac{1}{3\Gamma} \times w\xi . \quad (23)$$

These are only the leading terms in a series solution: higher order terms are needed if one wishes to extract, say, Cowling's function $\phi$: this is the function which Cowling (1941) uses in order to estimate the corrections to the eigenfrequencies due to perturbations in the gravitational potential.

We start the integrations of the oscillation equations by evaluating $w$ and $z$, using equations (19)–(23) at a fractional radius $f = 1.8 \times 10^{-4}$.

ii) *Surface Boundary Condition*

Using a trial frequency $\omega$, we integrate from the "center" to the "surface," and use a Newton-Raphson method to determine the eigenvalue, which causes the total pressure fluctuation to be zero at the perturbed boundary (cf. Ledoux and Walraven 1958). In terms of the variables in the present notation, the boundary condition is

$$w \times \theta^Q + (1 + n) \times \theta' \times z = 0 . \quad (24)$$

iii) *Number of Integration Steps*

For purposes of integration, we specify a parameter $N_{\rm loop}$ which is the number of points in the innermost loop of the eigenfunction. At each node, the radial step size is reduced in such a way that the number of points remains roughly constant in each loop, and equal (roughly) to $N_{\rm loop}$ throughout the star. An exception, however, is made in the outermost loop. Here, the number of points plays an important role in determining the precision of the eigenvalue, and its smooth approach to convergence. Therefore, we restrict the radial step size to be no larger than the radial grid spacing in the input polytrope table. With such a choice, we typically have several hundred grid points in the outermost loop. And typically half of these lie between the variable transition point $\xi_N$ and the boundary.

iv) *Range of Oscillation Frequencies*

In view of the observed concentration of power in the solar oscillations around periods of 5 minutes, we limited our search for eigenfrequencies to the range from 1700 to 5000 $\mu$Hz. For the polytrope $n = 3$, this allows us to determine eigenfrequencies for modes where the number of radial nodes varies from 12 to 37 (for $l = 2$). Since for polytropes of lower (higher) polytropic index, the frequency spacing between successive eigenmodes becomes greater (smaller) (see Table 1), by restricting our calculations to a particular frequency range in all cases, we are limited to fewer (more) modes for the polytropes with smaller (larger) indices.

For the spherical harmonic degree, we restrict our attention to the values $l = 0, 1, 2, 3$.

*d) Convergence Requirements*

Our aim is to increase both the size of the input polytrope table, $N_r$, and the number of integration steps per loop in the oscillation code, $N_{\rm loop}$, until the eigenfrequencies converge to better than 0.01 $\mu$Hz, and to ensure that the choice of the cutoff point, $\theta_0$, also has no further effect.

As an extreme example, we present in Table 2 the results we have obtained for the highest frequency mode with $l = 2$ for the $n = 3$ polytrope. (All values are for $\theta_0 = 10^{-7}$.) As regards the required number of points per loop, the approach to convergence seems to be essentially complete for $N_{\rm loop} = 50$. We shall use $N_{\rm loop} = 50$ in what follows.

As regards the value of $N_r$, extrapolation of the results on the last line of Table 2 suggests that a further doubling of $N_r$ beyond the largest value in Table 2 would increase the eigenfrequency by about 0.002 $\mu$Hz. Further doubling would result in an increase which is smaller by a further factor of 4–5. Such increases would not affect the eigenfrequency at the level of

TABLE 2

APPROACH OF EIGENVALUE TO CONVERGENCE

| | $N_r$ | | | |
|---|---|---|---|---|
| $N_{\rm loop}$ | 846 | 1706 | 3423 | 6852 |
| 10..... | 4898.617 | 4898.755 | 4898.782 | 4898.788 |
| 20..... | 4897.872 | 4898.013 | 4898.046 | 4898.054 |
| 30..... | 4897.831 | 4897.976 | 4898.009 | 4898.016 |
| 40..... | 4897.825 | 4897.969 | 4898.002 | 4898.010 |
| 50..... | 4897.822 | 4897.967 | 4898.000 | 4898.008 |
| 60..... | 4897.822 | 4897.967 | 4898.000 | 4898.008 |
| 70..... | 4897.822 | 4897.967 | 4898.000 | 4898.008 |

NOTE. Polytrope $n = 3$, $l = 2$. Units of frequency: $\mu$Hz. Standard frequency: 99.778 $\mu$Hz.

0.01 $\mu$Hz. Therefore, in what follows, we shall use $N_r = 6852$ for the $n = 3$ polytrope, and comparable values (6500–7500) for the other polytropes.

By way of reference, we note that for the last entry in Table 2 (with $N_{\rm loop} = 70$, $N_r = 6852$), the total number of radial steps in our oscillation code turns out to be 3913. Of these, 947 lie on the outermost loop of the eigenfunction, and 740 lie beyond the variable transition point radius $\xi_N$. For comparison, using the same value of $N_{\rm loop}$, but with $N_r = 1706$ (for which the eigenvalue is in error by 0.04 $\mu$Hz), the corresponding figures are 2657, 228, and 177. Thus, even with 228 points on the outermost loop, the eigenfunction is not precise at the level of 0.01 $\mu$Hz, at least for the choice of interpolation which we use (linear).

As regards the effects of varying the cutoff point, we may cite the example of the 12th-order $l = 2$ mode in the $n = 3$ polytrope. Using the shortest table of input values ($N_r = 847$), we find that the eigenvalue converges to 1796.886 $\mu$Hz for all values of $\theta_0$ between $10^{-7}$ and $10^{-4}$, but there is no convergence if $\theta_0$ is chosen to be as large as $10^{-3}$ and $10^{-2}$. For this particular mode, the variable transition point in fact lies at $\theta_N = 5.5 \times 10^{-4}$. Thus, the cutoff point must certainly be chosen to lie closer to the surface than $\xi_N$.

### *e) Testing of Polytrope Oscillation Code*

A standard test of a complete oscillation code (including perturbations to the gravitational potential $\phi$) is provided by comparing the eigenfrequencies for the $n = 0$ polytrope with the analytic values of Pekeris (1938). Although this is not strictly relevant for the Cowling approximation, an extension of the Pekeris treatment to the Cowling case has been provided by Sauvenier-Goffin (1951). (We acknowledge the assistance of an anonymous referee in this regard.) In Figure 1 we present the difference in frequency between our results for the $n = 0$ polytrope and the analytic predictions of Sauvenier-Goffin. (In plotting Fig. 1, we extended the frequency range to low values in order to include the three lowest order $p$-modes: this is the only figure where we will plot such low frequencies.) The differences between our frequencies and the analytic values are at most a few times 0.01 $\mu$Hz over the frequency range from 300 to 5000 $\mu$Hz. Thus, for present purposes, our numerical techniques seem to be satisfactory. The finite values of the differences in Figure 1 may be due to our truncation of the $n = 0$ polytrope at a rather large value of $\theta_0$ ($10^{-6}$).

For the polytrope $n = 3$, a comparison between our frequencies and those obtained from an independent code will be mentioned below (§ III*e*).

## III. RESULTS

We adopt the conventional manner of presenting the eigenfrequencies in the form of an echelle diagram (e.g., Fig. 2). In such a diagram, the spectrum is divided into segments of length $\Delta\nu$, starting at an arbitrary frequency $\nu_1$, and the segments are displayed vertically. Frequency increases downward and to the right.

Eigenfrequencies belonging to a particular $l$-value are symbolized in our echelle diagrams by the $l$-value. In plotting the

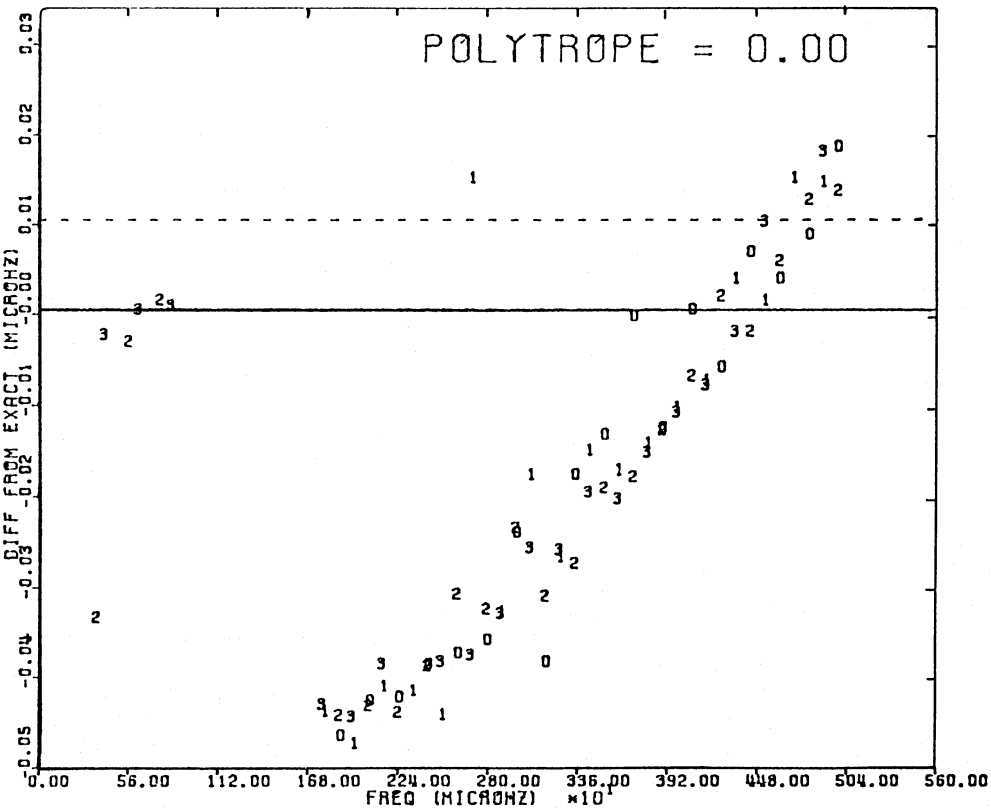


FIG. 1.—Differences between our mode frequencies for $n = 0$ polytrope and the analytic frequencies (from Sauvenier-Goffin 1951) as a function of frequency. Both axes are linear and are labeled in units of $\mu$Hz. Symbols denote the $l$-value of the mode, i.e., the spherical harmonic degree of the oscillation. The horizontal solid and dashed lines correspond to differences of zero and +0.01 $\mu$Hz, respectively.

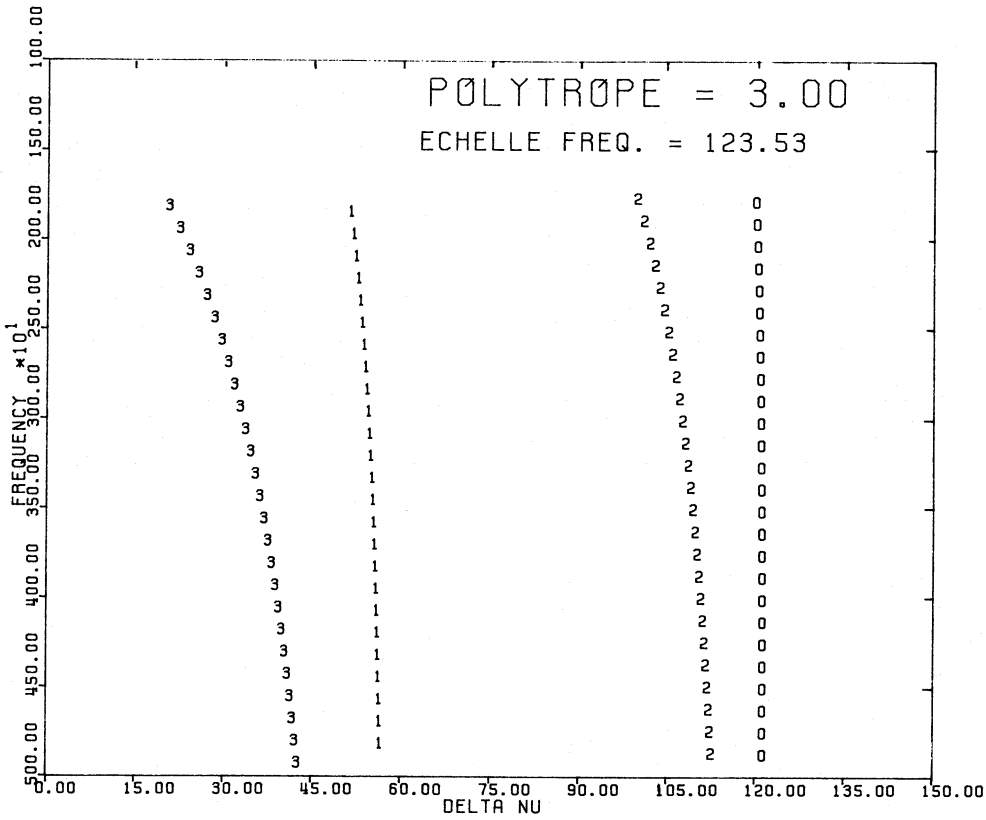


FIG. 2.—Echelle diagram for $n = 3$ polytrope. Frequency increases downward and to the right. Each segment of the plot has a length equal to the "echelle frequency" in the horizontal direction, and successive segments are displayed directly beneath one another. Units for both axes are $\mu$Hz. Symbols used to plot eigenfrequencies denote the $l$-value. The echelle frequency is chosen to be equal to $\beta_0(\theta_0)$ (Table 1).

diagrams, we have chosen as echelle frequency the value of $\beta_0(\theta_0)$ listed in Table 1.

### a) *Asymptotic Behavior: General*

The expected approach to asymptotic behavior is that the locus of eigenfrequencies for a particular $l$-value should become vertical toward the lower boundary if the echelle frequency has been chosen to be equal to $\beta$ for that $l$-value. In fact, the value of $\beta_1$ in equation (4) is sufficiently small that all four loci in the echelle diagram should become almost parallel as they approach the vertical asymptotes. Departures from vertical behavior arise from higher order terms in the asymptotic expansion. The approach to vertical behavior is apparent in Figure 2.

Echelle diagrams are characterized by two well-separated pairs of loci, one for $l = 3$ and $l = 1$, the other for $l = 2$ and $l = 0$. The separation between the two pairs is characterized by $\beta/2$, while within each pair, the splitting is characterized by $10(\alpha_1 - n_r\beta_1)$ and $6(\alpha_1 - n_r\beta_1)$ respectively (cf. eqs. [3] and [4]). (Here, $n_r$ is the radial mode number corresponding to the smaller value of $l$ in the pair.) Typical values of $\alpha_1$ and $\beta_1$ can be extracted from the results in Figure 2: at the highest frequencies we find 2.8 and 0.034 $\mu$Hz, respectively.

The example shown in Figure 2 is representative of the echelle diagrams which we have obtained for all values of the polytropic index $n \leq 3$: in all cases, the loci of constant-$l$ show curvature which is concave toward the left.

For higher values of the polytropic index, the echelle diagram at first retains its characteristic appearance (i.e., including four well-defined loci for the four $l$-modes), although the curvature reverses, and becomes concave towards the right (cf. Fig. 3 for the polytrope $n = 4.25$). However, as the polytropic index approaches the critical value of 5.0 (where the star has infinite radius), the characteristic appearance of the echelle diagram does not appear until the frequencies of the modes become quite high (cf. Fig. 4 for the polytrope $n = 4.5$). At low frequencies, the mode separations for $l = 1$, 2, and 3 in the $n = 4.5$ polytrope are so variable that it is difficult to recognize any pattern in the echelle diagram. However, at higher frequencies, the expected asymptotic behavior emerges. The $l = 0$ modes are an exception: their separations are close to asymptotic throughout our frequency range.

### b) *Odd-Even Splittings*

The splittings within the odd and even $l$-value loci in the echelle diagrams ($\Delta_{13}$ and $\Delta_{02}$) are expected to be in the ratio 10/6 if the modes follow the asymptotic behavior predicted by equations (3) and (4). Values of the odd and even splittings at our highest frequencies, and their ratio, are given in Table 3 for a number of polytropes. The approach to asymptotic behavior, based on this criterion, appears to be quite good for polytropic indices up to 3.5. For the higher order polytropes, it appears that we must go to frequencies in excess of 5000 $\mu$Hz before this particular aspect of asymptotic behavior is attained.

An expression for the splitting between even $l$-values is given by Cox, Guzik, and Kidman (CGK) (1987): the frequency dif-

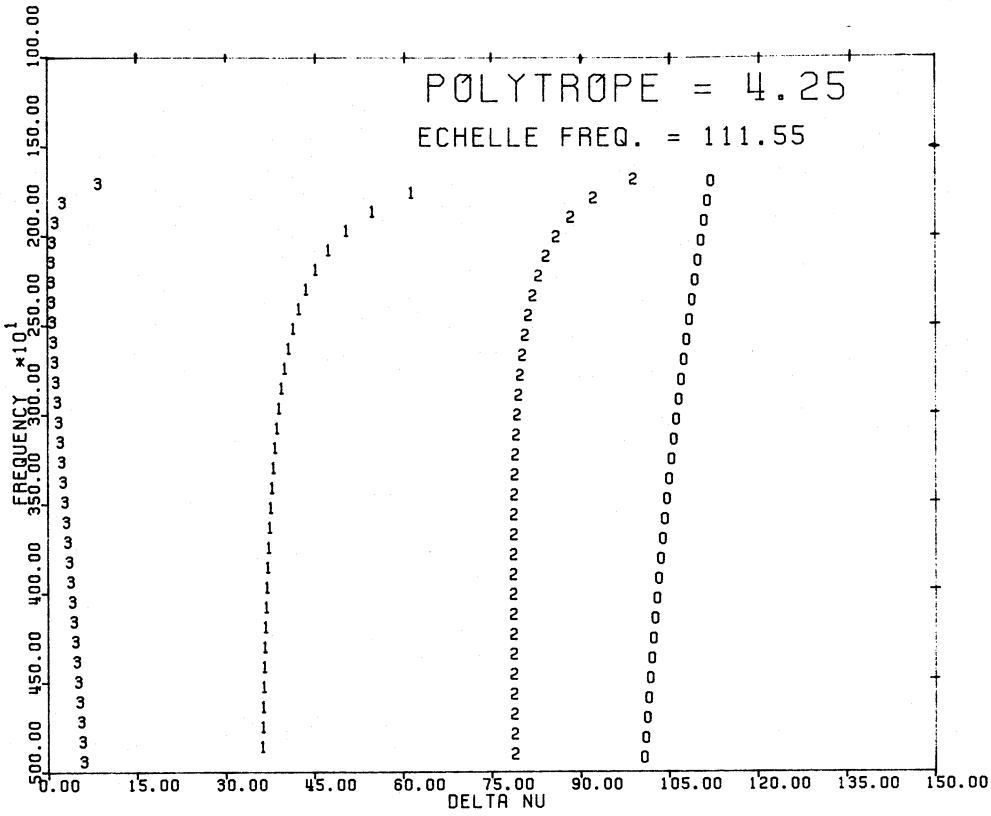


FIG. 3.—Same as Fig. 2 for $n = 4.25$

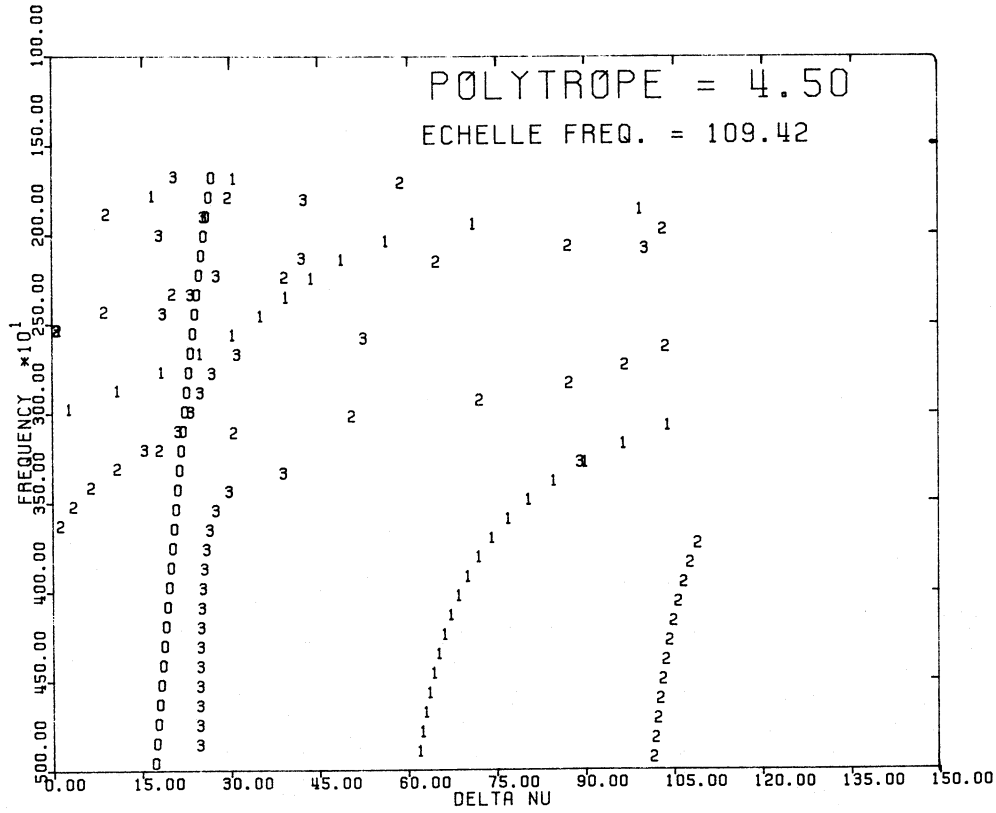


FIG. 4.—Same as Fig. 2 for $n = 4.5$

TABLE 3

ODD-EVEN SPLITTINGS OF MODE FREQUENCIES AT OUR HIGHEST FREQUENCIES

| Polytrope Index | $\Delta_{13}$ | $\Delta_{02}$ | $\frac{\Delta_{13}}{\Delta_{02}}$ | $\frac{\Delta_{02}}{\delta_{02}(\mathrm{CGK})}$ |
|---|---|---|---|---|
| 0.0 ..... | 8.52 | 5.02 | 1.70 | 0.99 |
| 1.0 ..... | 8.16 | 4.98 | 1.64 | 1.01 |
| 1.5 ..... | 8.69 | 5.30 | 1.64 | 1.00 |
| 2.0 ..... | 9.90 | 5.88 | 1.68 | 0.99 |
| 3.0 ..... | 14.40 | 8.68 | 1.66 | 0.94 |
| 3.25..... | 16.28 | 9.90 | 1.64 | 0.97 |
| 3.5 ..... | 18.68 | 11.52 | 1.62 | 0.89 |
| 4.0 ..... | 25.55 | 17.12 | 1.49 | 0.76 |
| 4.25..... | 30.37 | 21.85 | 1.39 | 0.65 |
| 4.5 ..... | 37.22 | 25.14 | 1.48 | 0.46 |

NOTE.—Units: $\mu$Hz. Standard frequency: 99.778 $\mu$Hz. Expected value of $\Delta_{13}/\Delta_{02}$ asymptotically is 1.67.

ference $\delta_{02}(\mathrm{CGK})$ between the $l = 0$ mode of order $n_r$ and the $l = 2$ mode of order $n_r - 1$ is

$$\delta_{02}(\mathrm{CGK}) = 6F/(n_r + 1)\,, \tag{25}$$

where the frequency $F$ is defined by

$$4\pi^2 F = \frac{c(R)}{R} - \int_0^R \frac{dc}{dr}\frac{dr}{r}\,. \tag{26}$$

Here, $c$ is the sound speed. The integral in equation (26) [to which we refer as $I(\mathrm{CGK})$] can be transformed in terms of the Lane-Emden function. For the polytrope $n = 0$, the integration yields $I(\mathrm{CGK}) = \pi/[2(6)^{1/2}]$ in units of $v_s$ (§ II*a* above); i.e. $I(\mathrm{CGK}) = \pi^2\beta_0(0)/2$, and $F = \beta_0(0)/8 = 22.77$ $\mu$Hz. For other values of the polytropic index, $n$, numerical integration indicates that with a cutoff at $\theta_0 = 10^{-8}$, the value of $I(\mathrm{CGK})$ (again in units of $v_s$) can be approximated remarkably well (to better than 1%) by a linear funtion of $n$:

$$I(\mathrm{CGK}) = 0.636 - 0.06 \times n\,. \tag{27}$$

In Table 3 we compare the even-mode splittings predicted by equation (25) with the values we have derived for $\Delta_{02}$. The predictions agree well with our values for the lower values of the polytropic index, but the predictions become too small as $n$ increases. Higher order corrections are needed in equation (25) for the higher $n$ values.

### c) *Asymptotic Behavior: Mode Separation*

It is worthwhile to examine in a more expanded manner how the asymptotic limit of frequency separations between adjacent modes is approached. The format which we choose for this purpose is to take the numerical difference between adjacent modes, $\Delta\nu_{n_r,n_r-1}$, and then derive the difference between this quantity and the predicted asymptotic value $\beta_0(\theta_0)$ (from Table 1).

Results for the polytrope $n = 3$ are presented in Figure 5. The abscissa is the mode frequency. Points are plotted with the appropriate $l$-value. The horizontal continuous line at an ordinate value of zero is the limit toward which all curves should

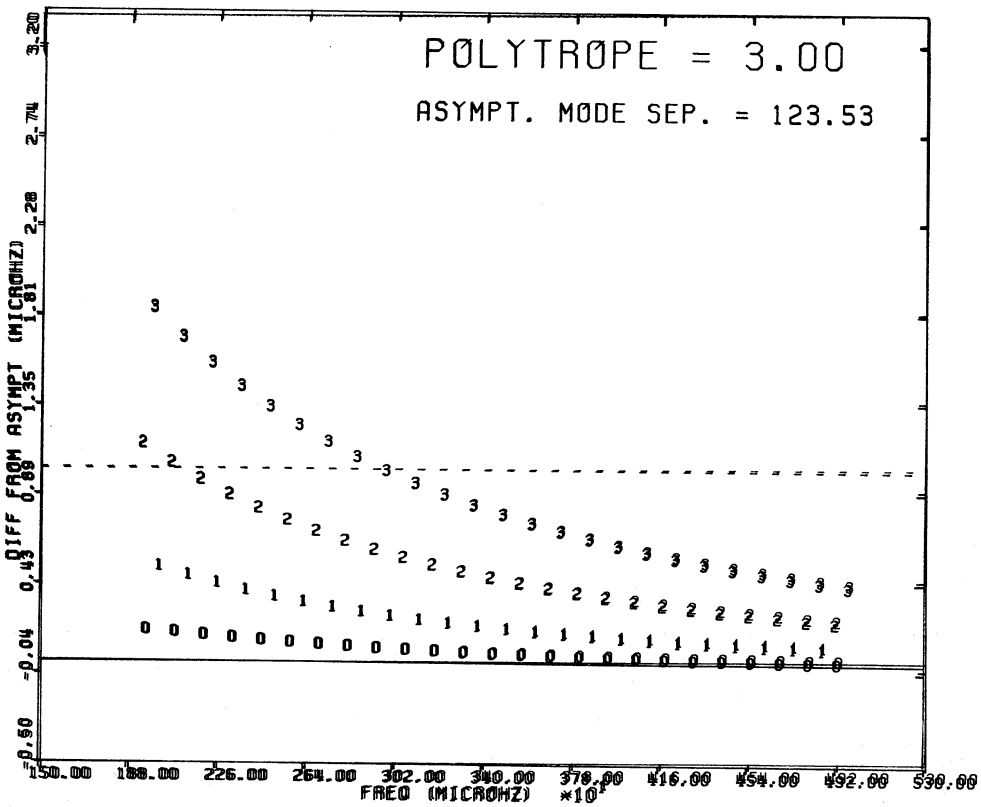


FIG. 5.—Frequency separation between adjacent modes as a function of frequency for polytrope $n = 3$. Abscissa shows the frequency of the eigenmodes (units of $\mu$Hz). Ordinate shows the difference (in $\mu$Hz) between the separation of adjacent modes and the asymptotic value $\beta_0(\theta_0)$ listed in Table 1. The latter is shown by a horizontal solid line. Horizontal dashed line indicates a difference of 1 $\mu$Hz relative to the asymptotic mode separation. The symbol used to plot each eigenmode is the $l$-value. Positive (negative) values of the ordinate in this figure correspond to leftward (rightward) concave curvature in Fig. 2.

converge according to Tassoul (1980). To provide a sense of the vertical scale of the plot, a horizontal dashed line is also plotted in the figure at an ordinate of $+1$ $\mu$Hz. Plotted points lying between the dashed line and the solid line have approached the asymptotic behavior to better than 1 $\mu$Hz.

For the polytrope $n = 3$, the results converge monotonically from above towards the expected value of $\beta_0(\theta_0)$. Clearly, for the lowest $l$-value, the approach to asymptotic behavior is already better than 0.1 $\mu$Hz even at the lowest order modes which we have considered. The two highest $l = 0$ modes which we have calculated are separated in frequency by 123.531 $\mu$Hz: this agrees to better than 0.01 $\mu$Hz with the predicted asymptotic value (see Table 1). Higher $l$-values require higher frequencies to approach asymptotic behavior. In accord with equation (4), the mode separations increase slightly for larger $l$-values. A value for the parameter $\beta_1$ can be extracted from our highest frequency points: for $n = 3$, we find $\beta_1 = 0.033$ $\mu$Hz. However, the exact numerical value of $\beta_1$ depends on which pair of $l$-values one uses, ranging from 0.033 to 0.036 $\mu$Hz.

As we decrease the order of the polytrope ($n = 2.0$, 1.5, and 1.0), we obtain the results which are shown in Figures 6–8. (The format is the same as in Fig. 5) Monotonic convergence from above appears in all of these, just as in $n = 3.0$. For $n = 0.0$ (Fig. 9), convergence from above again appears, but here, we find overshoot below the predicted asymptotic separation. We note, however, that the approach to convergence is not strictly monotonic. It is not clear why the results should be nonmonotonic only for the $n = 0.0$ case: it may be because of our unusually large choice of $\theta_0$ for this case ($10^{-6}$), or it may be because of numerical difficulties associated with the density step at the surface. The overshoot in Figure 9 may also occur for the same reasons.

Increasing the order of the polytrope ($n = 3.25$, 3.5, 4.0, 4.25, and 4.5) leads to the results which are shown in Figures 10–14. For these polytropes, uniform convergence from above is no longer the rule. Instead, we find, in the case of the lower $l$-values, convergence from below. The higher $l$-values show a nonmonotonic approach to asymptotic behavior. The alteration from convergence from above (for $n \leq 3$) to convergence from below (for $n \geq 3.5$) corresponds to the alteration from concave-left curvature in the echelle diagram (Fig. 2) to concave-right curvature (Fig. 3). The polytrope $n = 3.25$ appears to provide a transition between the two behaviors: for the $l = 0$ modes, the frequency separation between adjacent modes lies within 0.02 $\mu$Hz of the value of $\beta_0$ across our entire frequency range.

As a measure of the closeness of approach to asymptotic behavior, we list in Table 4 the difference (in $\mu$Hz) between the separation between our two highest $l = 0$ modes and the value of $\beta_0$. It appears that, at least for polytropes with $n \leq 3.5$, mode separations are within a few times 0.01 $\mu$Hz of the asymptotic values when the frequency of the modes has increased to 5000 $\mu$Hz. (An exception must be made for $n = 0$ because of numerical difficulties associated with the density step at the surface.) For higher order polytropes, the steep gradients of the physical variables inside the polytrope are such that we must go to higher frequencies before satisfactory approach to the asymptotic values is seen. Thus, steep density gradients either near the surface or near the center apparently make it more difficult to approach the asymptotic behavior predicted by Tassoul (1980).

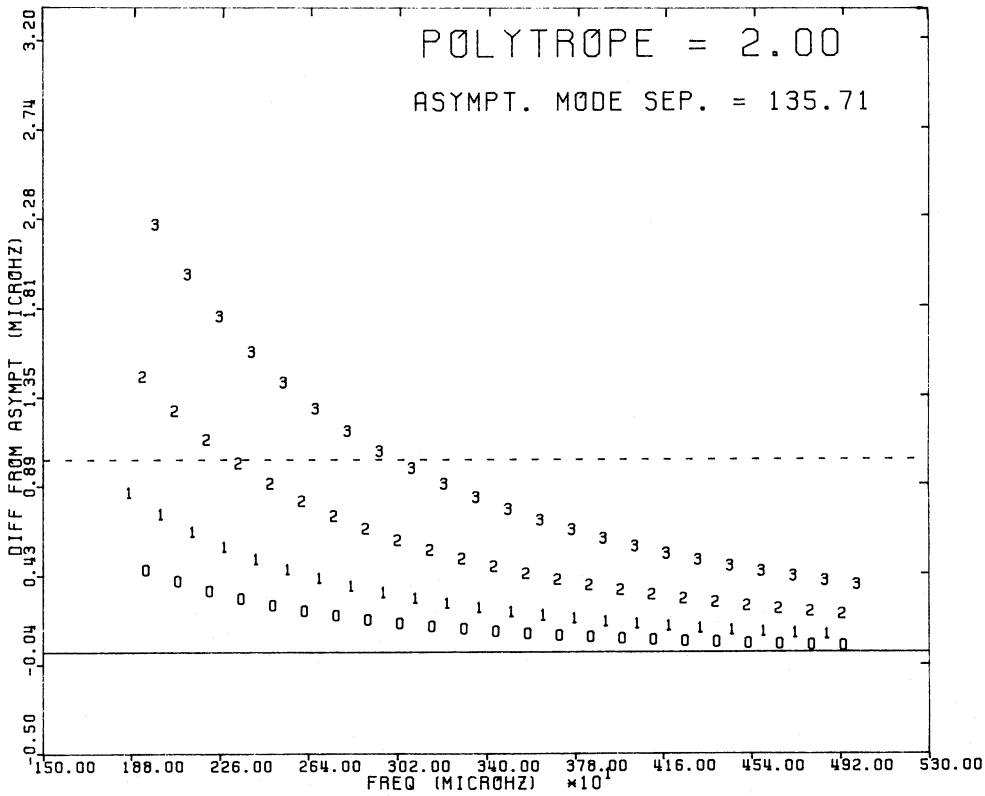


FIG. 6.—Same as Fig. 5 for $n = 2$

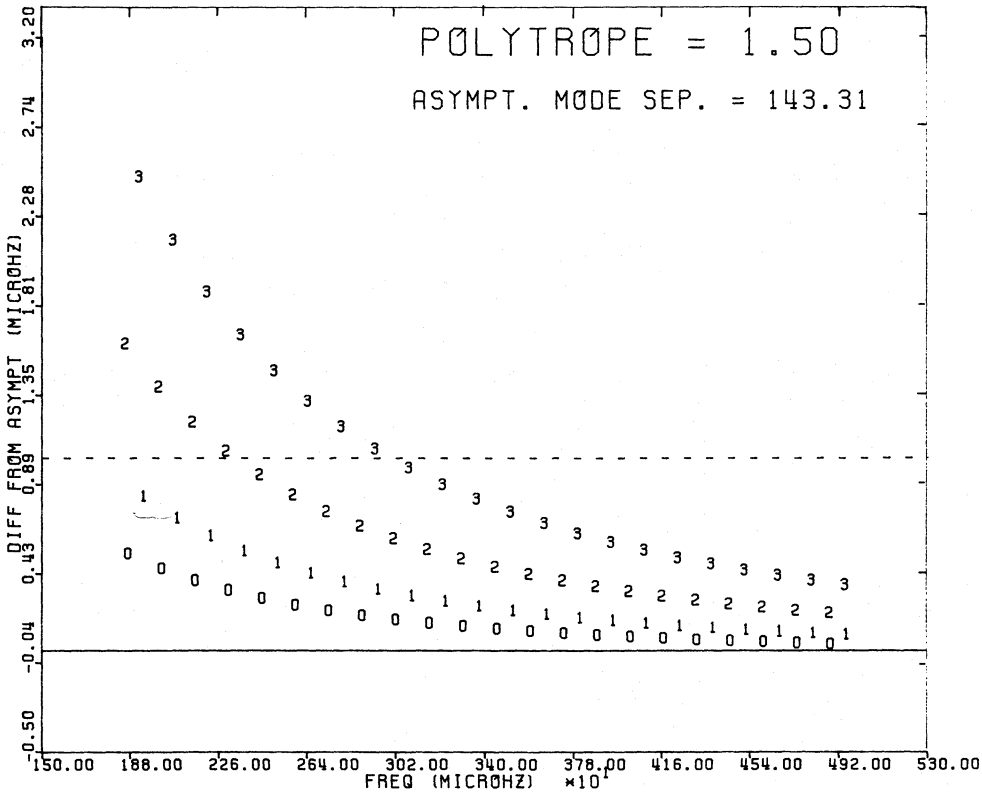


FIG. 7.—Same as Fig. 5 for $n = 1.5$

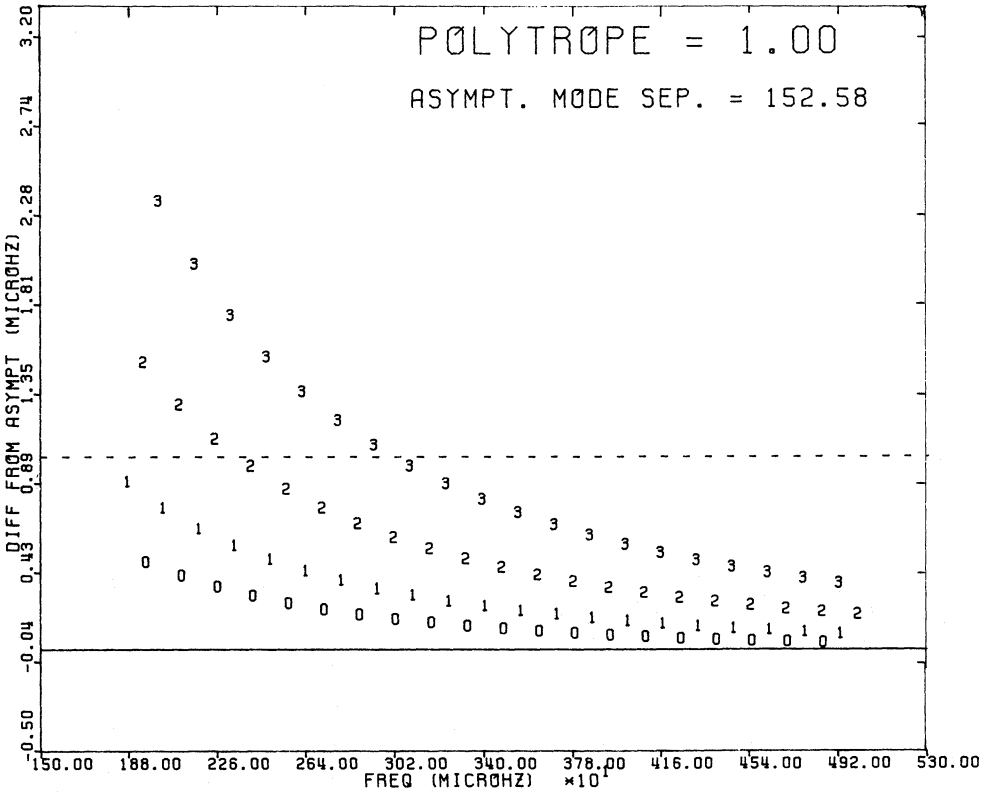


FIG. 8.—Same as Fig. 5 for $n = 1$

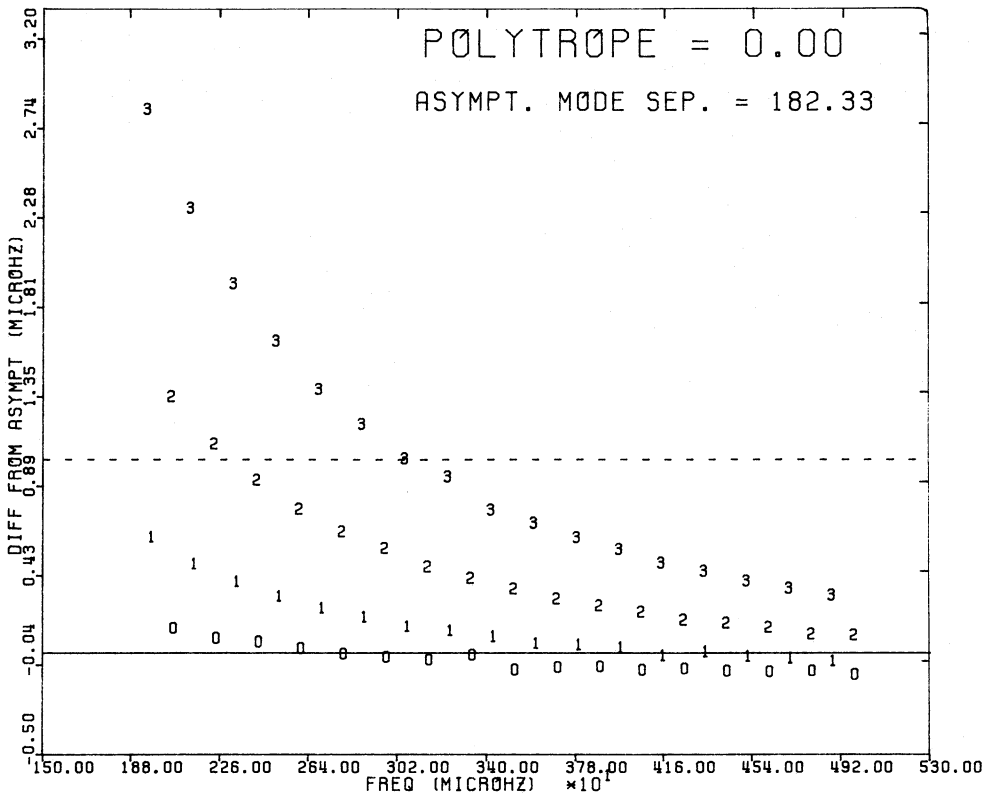


FIG. 9.—Same as Fig. 5 for $n = 0$. Numerical difficulties may be responsible for the lack of monotonic behavior in this case.

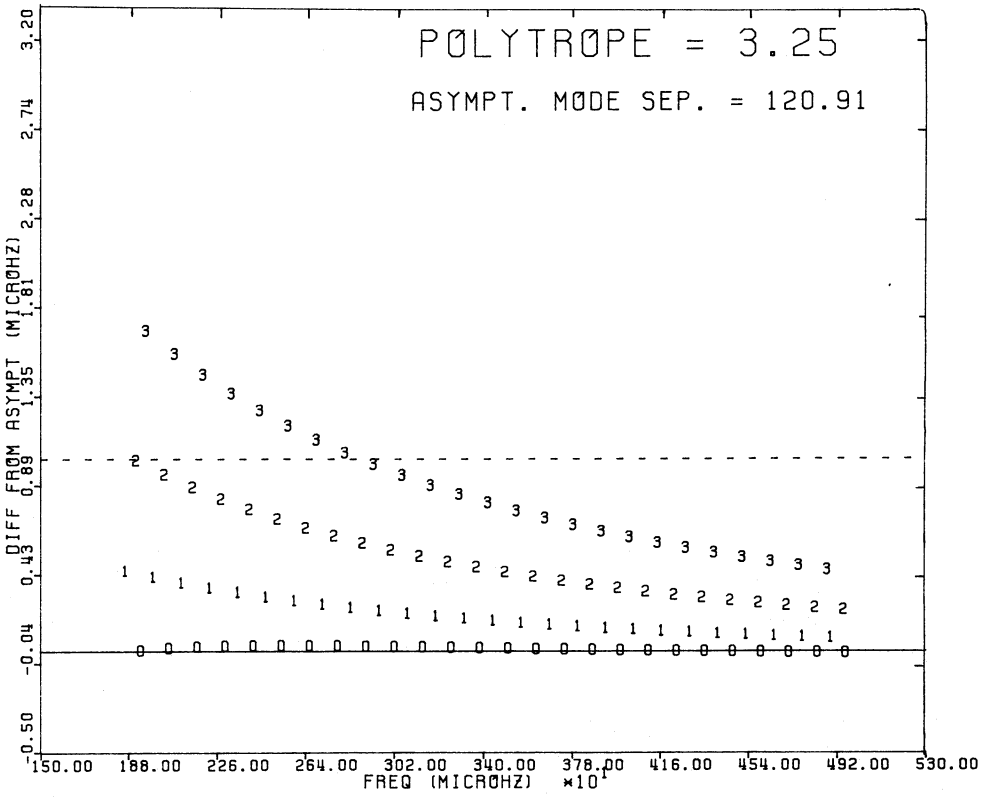


FIG. 10.—Same as Fig. 5 for $n = 3.25$

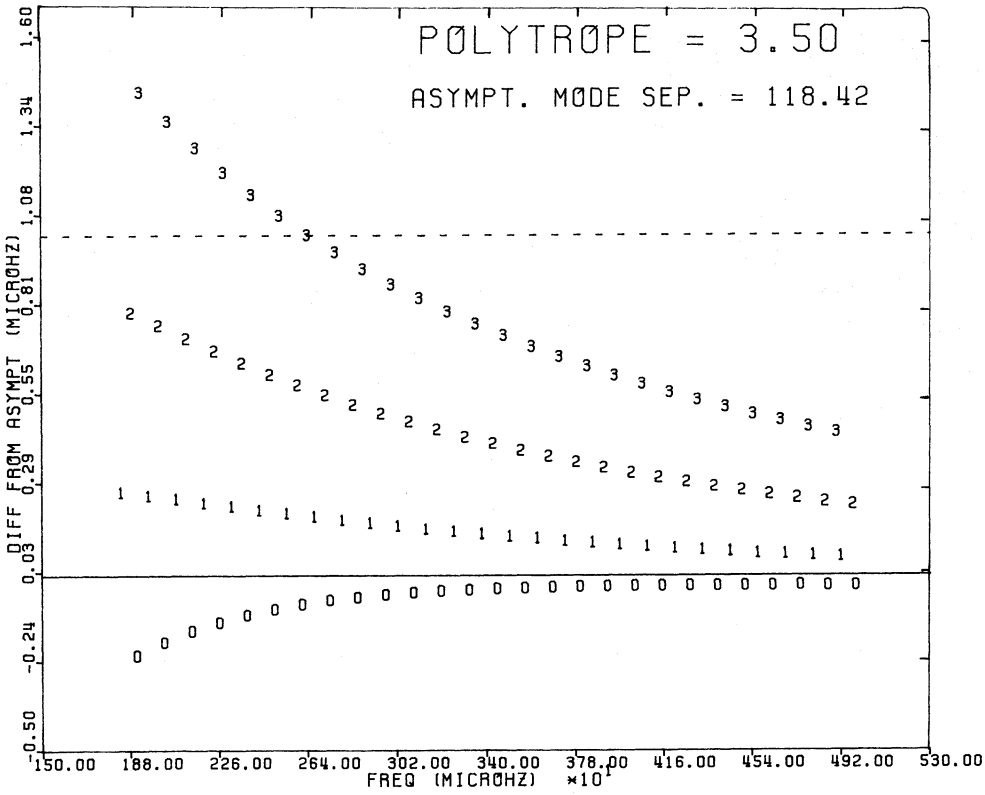


FIG. 11.—Same as Fig. 5 for $n = 3.5$

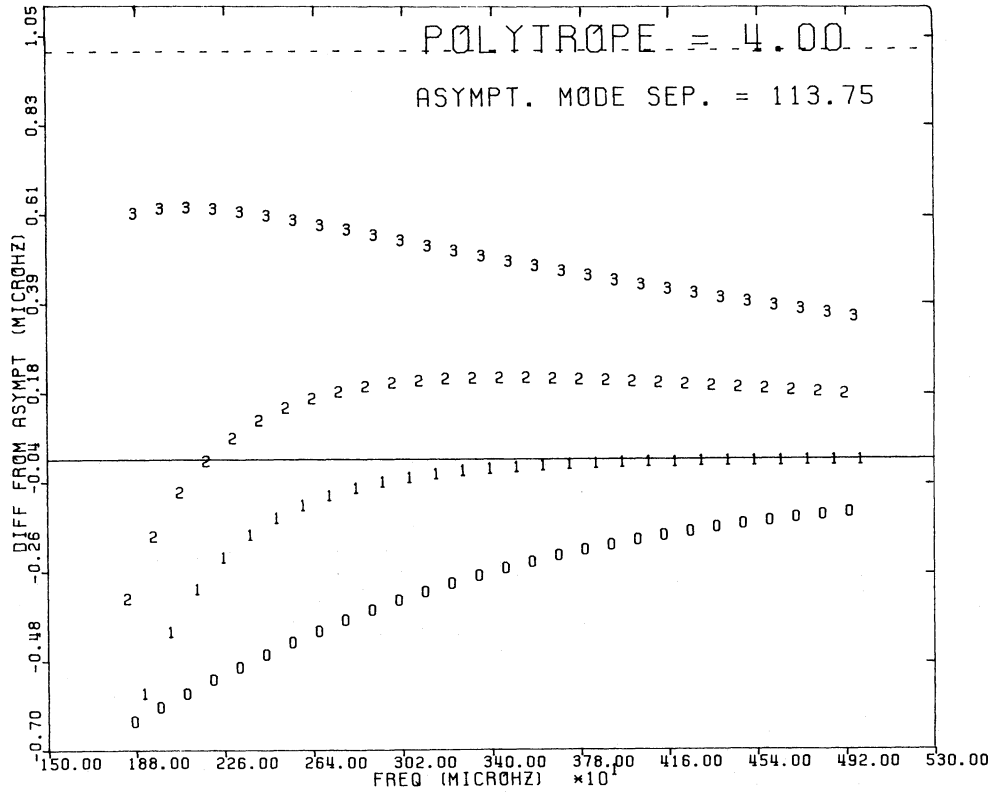


FIG. 12.—Same as Fig. 5 for $n = 4$

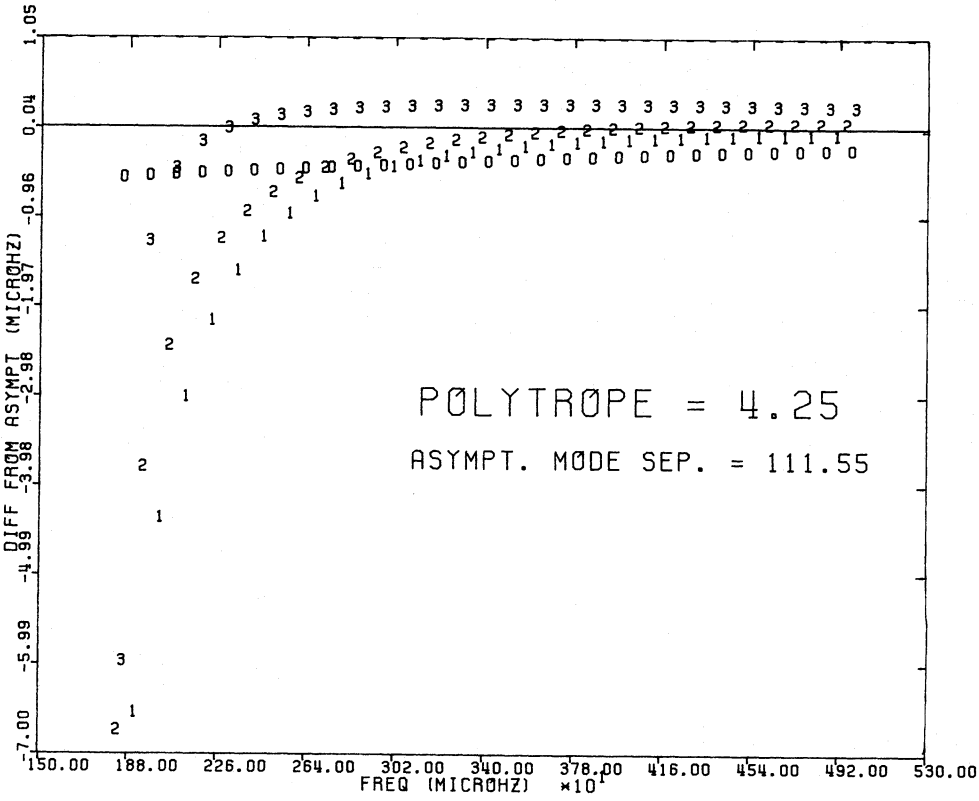


FIG. 13.—Same as Fig. 5 for $n = 4.25$

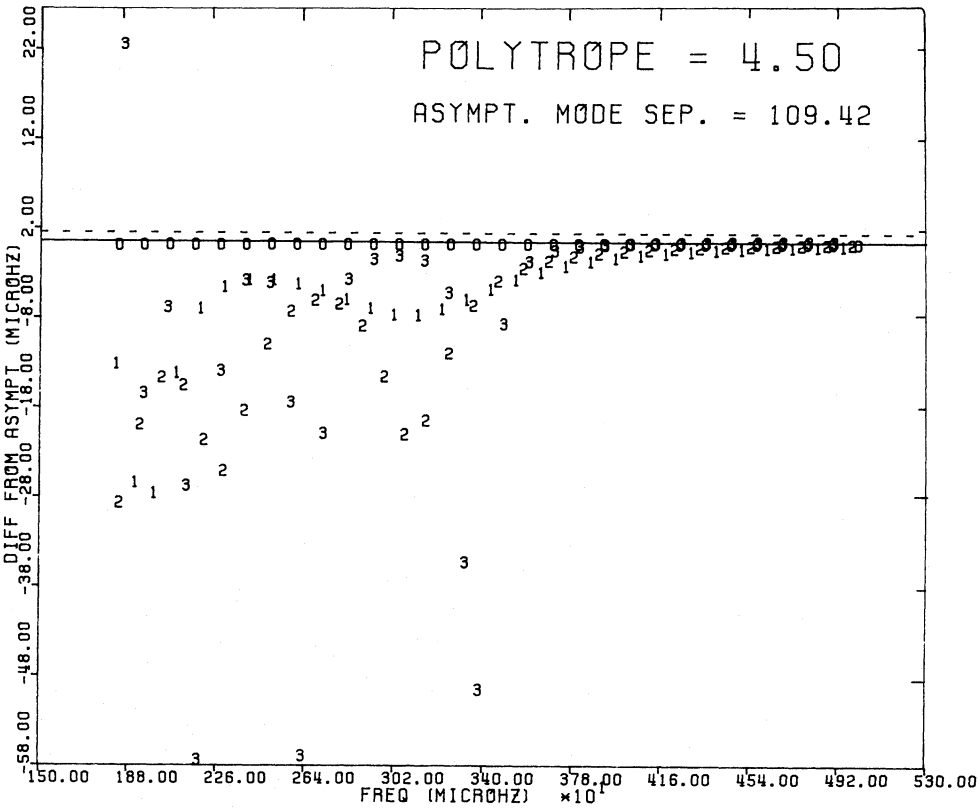


FIG. 14.—Same as Fig. 5 for $n = 4.5$

TABLE 4

DEVIATION BETWEEN SEPARATION OF OUR TWO HIGHEST $l = 0$ MODES AND THE ASYMPTOTIC PREDICTION $\beta_0(\theta_0)$

| Polytrope Index | Deviation |
|---|---|
| +0.00 | −0.12 |
| +1.00 | +0.03 |
| +1.50 | +0.03 |
| +2.00 | +0.03 |
| +3.00 | +0.00 |
| +3.25 | −0.01 |
| +3.50 | −0.03 |
| +4.00 | −0.13 |
| +4.25 | −0.24 |
| +4.50 | −0.26 |

NOTE—Units: μHz. Standard frequency: 99.778 μHz.

*d) Tabulated Eigenfrequencies for n = 3 and n = 1.5*

For reference, we provide in Tables 5 and 6 the eigenfrequencies of all modes with $l = 0$–3 which lie between 1700 and 5000 μHz for the polytropes $n = 3$ and $n = 1.5$. The central condensations in these two polytropes are sufficiently small (Scuflaire 1974) that for $l = 1$–3, the radial order equals the number of zeroes in the radial displacement eigenfunction. For $l = 0$, the radial order exceeds by unity the number of zeroes in the radial displacement eigenfunction (cf. Cox 1980, p. 239).

TABLE 5

EIGENVALUES (IN μHz) OF HIGH-ORDER $p$-MODES IN $n = 3$ POLYTROPE

| | $l$ | | | |
|---|---|---|---|---|
| $n_r$[a] | 0 | 1 | 2 | 3 |
| 11 | ... | ... | ... | 1715.762 |
| 12 | ... | 1748.030 | 1796.926 | 1841.285 |
| 13 | 1817.019 | 1872.101 | 1921.580 | 1966.638 |
| 14 | 1940.709 | 1996.120 | 2046.134 | 2091.840 |
| 15 | 2064.386 | 2120.094 | 2170.601 | 2216.910 |
| 16 | 2188.049 | 2244.028 | 2294.990 | 2341.860 |
| 17 | 2311.699 | 2367.927 | 2419.310 | 2466.705 |
| 18 | 2435.338 | 2491.793 | 2543.570 | 2591.455 |
| 19 | 2558.966 | 2615.631 | 2667.773 | 2716.120 |
| 20 | 2682.583 | 2739.444 | 2791.927 | 2840.708 |
| 21 | 2806.192 | 2863.234 | 2916.036 | 2965.225 |
| 22 | 2929.792 | 2987.002 | 3040.104 | 3089.677 |
| 23 | 3053.385 | 3110.752 | 3164.135 | 3214.072 |
| 24 | 3176.971 | 3234.484 | 3288.132 | 3338.412 |
| 25 | 3300.551 | 3358.202 | 3412.098 | 3462.705 |
| 26 | 3424.124 | 3481.905 | 3536.037 | 3586.951 |
| 27 | 3547.693 | 3605.595 | 3659.948 | 3711.157 |
| 28 | 3671.256 | 3729.273 | 3783.836 | 3835.324 |
| 29 | 3794.814 | 3852.940 | 3907.702 | 3959.455 |
| 30 | 3918.368 | 3976.596 | 4031.547 | 4083.552 |
| 31 | 4041.919 | 4100.245 | 4155.374 | 4207.620 |
| 32 | 4165.466 | 4223.883 | 4279.183 | 4331.660 |
| 33 | 4289.009 | 4347.514 | 4402.976 | 4455.673 |
| 34 | 4412.551 | 4471.138 | 4526.754 | 4579.662 |
| 35 | 4536.089 | 4594.755 | 4650.519 | 4703.626 |
| 36 | 4659.624 | 4718.366 | 4774.270 | 4827.571 |
| 37 | 4783.157 | 4841.970 | 4898.008 | 4951.495 |
| 38 | 4906.688 | ... | ... | ... |

NOTE.—Standard frequency: 99.778 μHz.
[a] Radial order of the mode.

TABLE 6

EIGENFREQUENCIES (IN μHz) OF HIGH-ORDER $p$-MODES IN $n = 1.5$ POLYTROPE

| | $l$ | | | |
|---|---|---|---|---|
| $n_r$[a] | 0 | 1 | 2 | 3 |
| 10 | ... | ... | 1697.436 | 1755.922 |
| 11 | 1712.151 | 1779.333 | 1842.337 | 1901.686 |
| 12 | 1855.964 | 1923.444 | 1987.012 | 2047.121 |
| 13 | 1999.699 | 2067.442 | 2131.506 | 2192.289 |
| 14 | 2143.371 | 2211.347 | 2275.851 | 2337.235 |
| 15 | 2286.994 | 2355.175 | 2420.072 | 2481.995 |
| 16 | 2430.574 | 2498.940 | 2564.188 | 2626.598 |
| 17 | 2574.120 | 2642.652 | 2708.218 | 2771.069 |
| 18 | 2717.637 | 2786.320 | 2852.173 | 2915.426 |
| 19 | 2861.128 | 2929.948 | 2996.064 | 3059.683 |
| 20 | 3004.599 | 3073.544 | 3139.899 | 3203.854 |
| 21 | 3148.052 | 3217.110 | 3283.685 | 3347.951 |
| 22 | 3291.488 | 3360.652 | 3427.429 | 3491.981 |
| 23 | 3434.911 | 3504.171 | 3571.135 | 3635.951 |
| 24 | 3578.321 | 3647.670 | 3714.808 | 3779.869 |
| 25 | 3721.719 | 3791.152 | 3858.451 | 3923.741 |
| 26 | 3865.109 | 3934.619 | 4002.068 | 4067.572 |
| 27 | 4008.490 | 4078.072 | 4145.660 | 4211.364 |
| 28 | 4151.864 | 4221.512 | 4289.232 | 4355.123 |
| 29 | 4295.229 | 4364.941 | 4432.783 | 4498.850 |
| 30 | 4438.589 | 4508.360 | 4576.318 | 4642.551 |
| 31 | 4581.944 | 4651.771 | 4719.835 | 4786.225 |
| 32 | 4725.293 | 4795.172 | 4863.340 | 4929.875 |
| 33 | 4868.635 | 4938.566 | ... | ... |

NOTE.—Standard frequency: 99.778 μHz.
[a] Radial order of the mode.

*e) Comparison with n = 3 Results from an Independent Code*

Over the last few years, one of us (R. K. U.) has independently developed an oscillation code for extracting eigenfrequencies from realistic solar models. This code incorporates the ability to switch the gravitational potential perturbations on or off. In order to compare with the results obtained in the present paper, this code has been run in the "switch-off" mode for the $n = 3$ polytrope.

In the first instance, the code was run with 574 radial zones: this is close to what is used when the full code (including "switch-on") is applied to standard solar models. Eigenfrequencies were extracted for $l$-values of 0–3, and for modes up to radial order $n_r = 32$. We refer to this set of eigenfrequencies as $U574$. Differences between the results obtained in the present paper and $U574$ are presented in Figure 15. At frequencies below about 3000 μHz, the differences for $l = 2$ and $l = 3$ are very small, averaging 0.01 μHz in absolute value. For $l = 1$ and $l = 0$, the differences at the lower frequencies are on average a few times 0.01 μHz. At higher frequencies, the differences increase to 0.1–0.2 μHz.

In the second instance, the "switch-off" code was run with 780 radial zones. Of these, 150 are situated between $r = 0.99R$ and $R$. There are about 80 zones in the outermost loop of the eigenfunction, and (for the higher order modes) about 20 zones in the loops in the interior. Frequencies obtained with this code are referred to as $U780$. Differences between present results and $U780$ are shown in Figure 16. For $l = 1$, 2, and 3, the absolute differences are smaller than for $U574$, although the divergence above 0.1 μHz persists at the higher frequencies. For $l = 0$, the differences become larger than 0.2 μHz at the higher frequencies.

These results support our previous conclusion that many

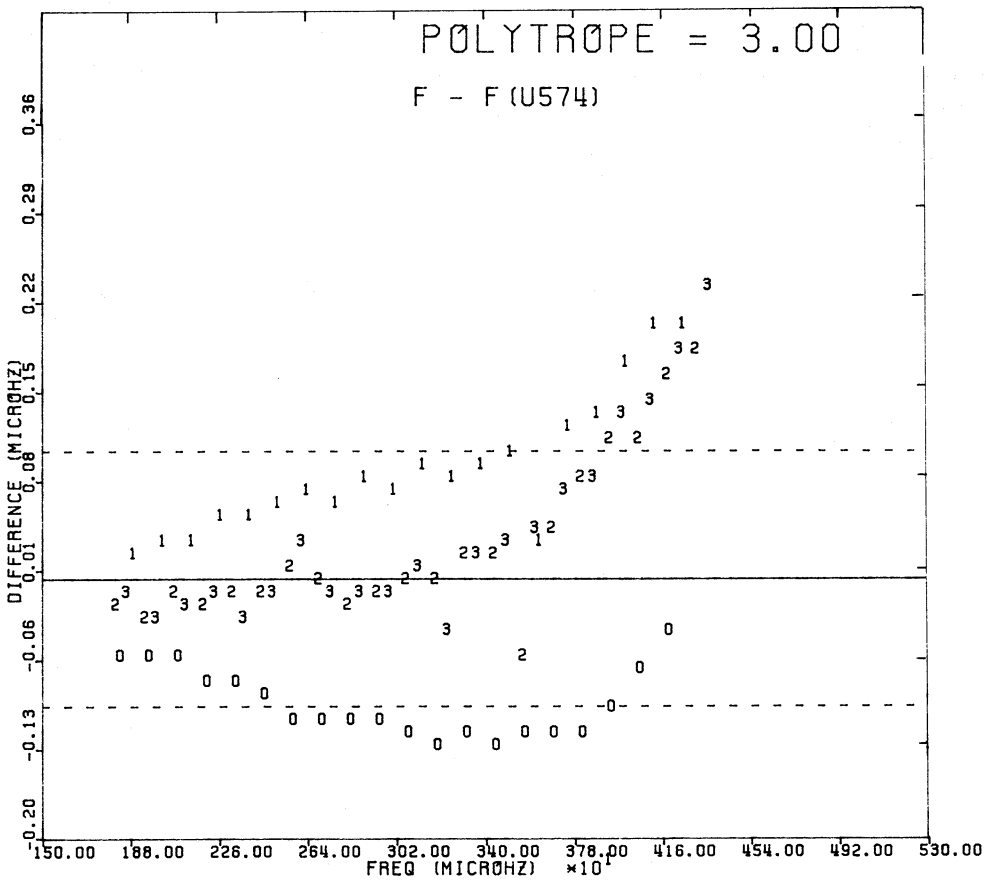


FIG. 15.—Differences between frequencies for the $n = 3$ polytrope obtained in the present paper and those obtained by an independent code developed by one of us (R. K. U.), using 574 radial zones and no gravitational potential perturbation. Horizontal continuous line denotes zero difference. Horizontal dashed lines denote differences of $\pm 0.1$ $\mu$Hz. Symbols denote $l$-value.

radial zones are required in the outermost loop of the eigenfunctions if the frequencies are to be obtained with a precision of 0.01 $\mu$Hz.

## IV. SUMMARY AND CONCLUSIONS

We have obtained eigenfrequencies for high-order radial and nonradial $p$-mode pulsations in polytropes in the Cowling approximation. Our aim has been to obtain the eigenfrequencies in the frequency range 1700–5000 $\mu$Hz with a precision of 0.01 $\mu$Hz. In presenting our results, we have used mass and radius equal to solar values, with a "standard frequency" (cf. eq. [10]) of 99.778 $\mu$Hz.

A careful treatment of the central and surface regions has been included: near the center, we use only the dominant terms in a series expansion of the solutions of the oscillation equations, and near the surface, several hundred grid points are used across the outermost loop of the eigenfunction. We have examined the polytropes $n = 0$, 1, 1.5, 2, 3, 3.25, 3.5, 4, 4.25, and 4.5. Characteristic frequencies associated with sound-wave crossing times are listed for these polytropes in Table 1.

We have used our results to examine the approach to the asymptotic behavior discussed by Tassoul (1980). We find that the frequency differences between successive eigenmodes converge qualitatively as expected. And for polytropes $n = 3$ and $n = 3.25$, the convergence is also quantitatively satisfactory within 0.01 $\mu$Hz. However, for the other polytropes which we have considered, we find that the approach to asymptotic separations is in general not as good as 0.01 $\mu$Hz even for the highest order modes we have considered (radial order about 40) (see Table 4). Moreover, the direction of convergence is opposite for the polytropes with large index from that for the polytropes with small index: this occurs presumably because of higher order corrections to Tassoul's predictions.

The work in the present paper has been restricted to the Cowling approximation, as if the polytropic stars had somehow switched off their gravitational potential perturbations. In a subsequent paper, we plan to extend the present work by comparing the exact frequencies (obtained without using the Cowling approximation) with the asymptotic approximations.

D. J. M. wishes to thank Dr. Charles Wolff for insightful comments which were key to obtaining some of the results presented here. He also thanks Dr. Dean Pesnell and Dr. J. Christensen-Dalsgaard for providing eigenfrequencies for their polytrope models. The comments of an anonymous referee are appreciated, especially with respect to the work of Sauvenier-Goffin.

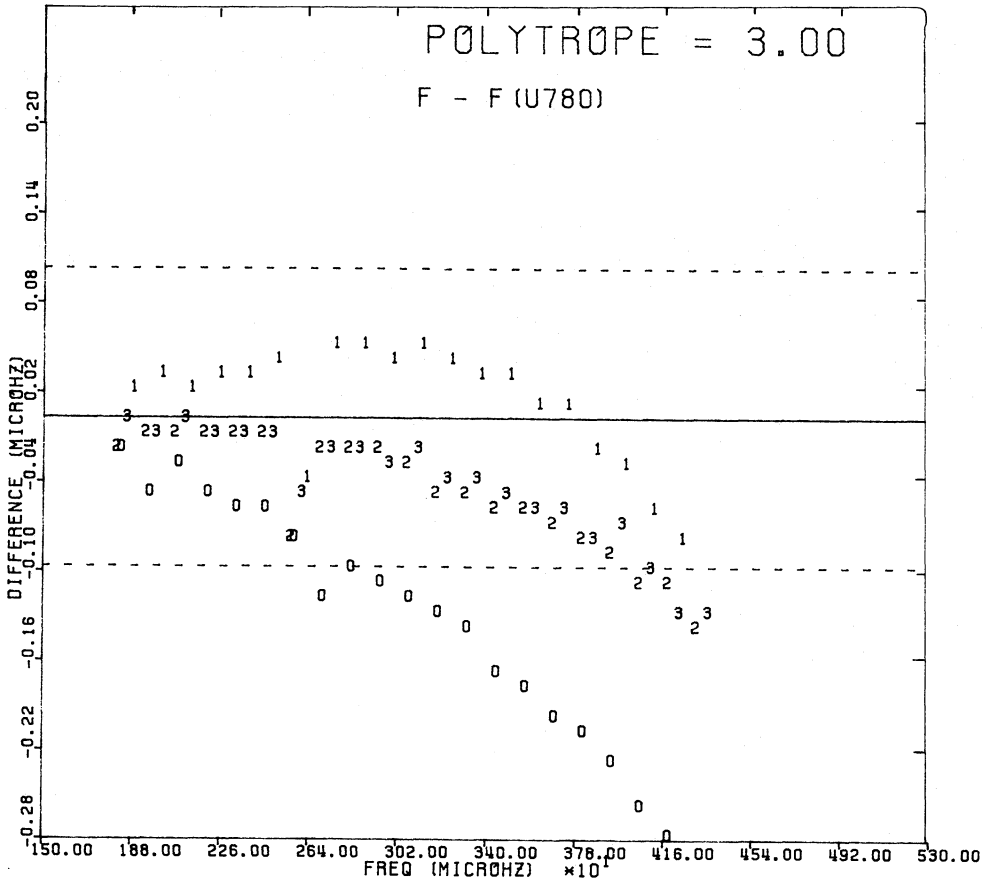


FIG. 16.—Same as Fig. 15 for a model of $n = 3$ polytrope with 780 radial zones

## REFERENCES


Chandrawekhar, S. 1939, *An Introduction to the Study of Stellar Structure* (New York: Dover), p. 83.
Christiansen-Dalsgaard, J. 1982, *M.N.R.A.S.*, **199**, 735.
Cox, A. N., Guzik, A., and Kidman, R. B. 1987, preprint (CGK).
Cox, J. P. 1980, *Theory of Stellar Pulsation* (Princeton: Princeton University Press), pp. 242–245.
Cowling, T. G. 1941, *M.N.R.A.S.*, **101**, 367.
Gough, D. O. 1984, *Adv. Space Res.*, Vol. **4**, No. 8, p. 91.
Ledoux, P., and Walraven, T. 1958, in *Handbuch der Physik*, Vol. **51**, ed. S. Flügge (New York: Springer), p. 515.
Pekeris, C. L. 1938, *Ap. J.*, **88**, 189.
Robe, H. 1968, *Ann. d'Ap.*, **31**, 475.
Sauvenier-Goffin, E. 1951, *Bull. Soc. Roy. Sci. Liège*, **20**, 20.
Scuflaire, R. 1974, *Astr. Ap.*, **36**, 107.
Smeyers, P., and Tassoul, M. 1987, *Ap. J. Suppl.*, **65**, 429.
Tassoul, M. 1980, *Ap. J. Suppl.*, **43**, 469.
Unno, W., Osaki, Y., Ando, H., and Shibahashi, H. 1981, *Nonradial Oscillations of Stars* (Tokyo: University of Tokyo Press), p. 11.



D. J. MULLAN: Bartol Research Institute, University of Delaware, Newark DE 19716

R. K. ULRICH: Astronomy Department, University of California, 8931 MSB, Los Angeles CA 90024